Highly nonlinear yttrium-aluminosilicate optical fiber with high intrinsic stimulated Brillouin scattering threshold

M. Tuggle,[1] C. Kucera,[1] T. Hawkins,[1] D. Sligh,[1] A. F. J. Runge,[2] A. C. Peacock,[2] P. Dragic,[3] and J. Ballato[1,*]

[1]*Center for Optical Materials Science and Engineering Technologies (COMSET) and the department of Materials Science and Engineering, Clemson University, Clemson, SC, 29625*
[2]*Optoelectronics Research Centre, University of Southampton, Highfield, Southampton, Hampshire SO17 IBJ, UK*
[3]*Department of Electrical and Computer Engineering, University of Illinois at Urbana, Champaign, Urbana, IL 61822*
**Corresponding author: jballat@clemson.edu*

Received XX Month XXXX; revised XX Month, XXXX; accepted XX Month XXXX; posted XX Month XXXX (Doc. ID XXXXX); published XX Month XXXX

Highly nonlinear (high-NA small-mode-area) optical fibers also possessing intrinsically high stimulated Brillouin scattering (SBS) threshold are described. More specifically, silica clad, yttrium-aluminosilicate core fibers are shown to exhibit an intrinsically low Brillouin gain coefficient between 0.125 and 0.139 × 10^{-11} m/W, and a Brillouin gain linewidth of up to 500 MHz. Losses on the order of 0.7 dB/m were measured, resulting from impurities in the precursor materials. Nonlinear refractive index values are determined to be similar to that of silica, but significant measurement uncertainty is attributed to the need to estimate dispersion curves since their direct measurement could not be made. The interest for highly nonlinear optical fibers with a low intrinsic Brillouin gain coefficient is expected to continue, especially with the growing developments of narrow-linewidth high energy laser systems.

OCIS codes: *(060.0060) Fiber optics and optical communications; (060.2290) Fiber materials; (060.3510) Lasers, fiber; (060.4370) Nonlinear optics, fiber; (290.5830) Scattering, Brillouin*

http://dx.doi.org/10.1364/OL.99.099999

Nonlinear optical fibers are useful for a wide range of modern photonic devices including Raman [1] and parametric [2] amplifiers as well as supercontinuum sources [3]. However, the signal spectrum required to induce such nonlinearities often leads to stimulated Brillouin scattering (SBS), which limits scaling to higher power levels. Popular approaches to suppress SBS include phase modulation of the signal [4], the application of strain along the fiber [5], and segmentation of the fiber [6]. These active means of SBS suppression notwithstanding, a practical passive approach is most desirable. An example of this latter case are acoustic anti-guiding designs [7,8], which employ alumina (Al_2O_3) as a dopant into the core. Alumina is known to raise the acoustic velocity when added to pure silica (SiO_2) [9] and, thus, the acoustic wave can be compositionally engineered to have large waveguide attenuation due to modes that radiate away from the (acoustic) anti-wave-guiding core [10].

Such a passive materials-approach to SBS mitigation has proven more effective than that of aforementioned active methods [10]. The basic concept is that the Brillouin gain coefficient, (BGC), is proportional to the square of the Pockels photoelastic coefficient, p_{12}. Accordingly, the addition of a material to silica ($p_{12} > 0$) that possesses a negative p_{12} value, such as BaO, SrO, MgO, and Al_2O_3, can yield substantial reductions in the effective p_{12} value. This includes the not-yet-realized potential for $p_{12} = 0$ where Brillouin scattering would be entirely negated [11]. Accordingly, the beauty of Al_2O_3 as a dopant into silica is that the aluminosilicate glass exhibits both a reduced p_{12} value and a large material acoustic attenuation coefficient, hence acoustic anti-wave-guidance.

Unfortunately, the alumina concentration required to significantly impact p_{12} is not tenable using conventional fiber fabrication methods [12]. Accordingly, the molten core approach has been utilized to achieve fibers possessing up to 50 mole% Al_2O_3 [11]. Additionally, acoustic anti-guidance is only relevant when the waveguide attenuation term is comparable to the material damping coefficient [10], the former being a strong function of the core diameter and its acoustic velocity relative to the silica cladding [13]. As such, to better control the acoustic velocity increase due to the alumina, a velocity-reducing additive must also be incorporated. As discussed in detail below, this is achieved by a novel multilayered molten core fabrication process wherein an inner YAG rod is surrounded by a sapphire sleeve. Through careful selection of the relative sizes of these single crystal elements, the relative concentration of Al_2O_3 (from the Al_2O_3 sleeve and from the YAG precursor) and Y_2O_3 (from the YAG precursor)

in the melt, and therefore the acoustic velocity and refractive index of the subsequent all-glass core, can be tailored. It is shown that highly nonlinear fibers can be realized with Brillouin spectra broader than those obtained by straining optical fiber [2], with one fiber exhibiting a spectrum spread across roughly 500 MHz.

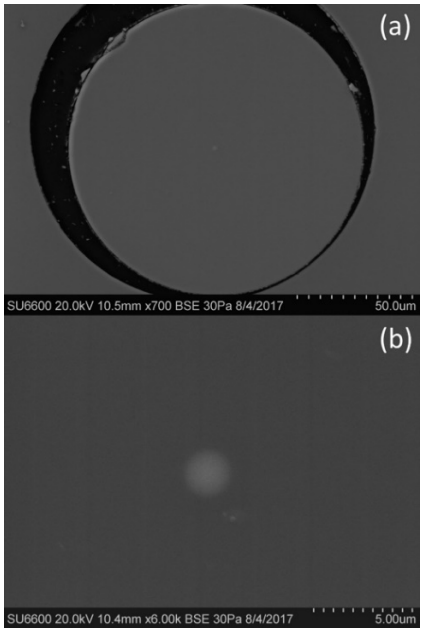

Fig. 1. SEM micrograph of Fiber 2 (a) in epoxy, and (b) of the core.

Optical fibers were produced using the molten core method of fiber fabrication [12]. Specifically, a 1 mm outer diameter Yb:YAG rod (Roditi International, London) was sleeved inside of a 1.1 mm inner diameter / 1.5 mm outer diameter sapphire (Al_2O_3) sleeve (Saint-Gobain). For completeness, it is noted that the ytterbium doping plays no specific role in this particular Letter. Its use is for subsequent investigations of active low-SBS fibers. This precursor core then was inserted into a telecommunications-grade silica capillary preform (3 mm inner diameter / 30 mm outer diameter) that served as the cladding for the fiber, which was drawn at 2000°C. The primary purpose of the alumina sleeve was to investigate whether or not an intermediate cladding would lessen the incorporation of silica from the cladding into the core, as is typical of molten core derived oxide glass fibers. A secondary purpose for the sleeve was to increase the Al_2O_3 content in the core, since alumina is known to reduce the BGC [11]. Due to the high cooling rates of the fiber draw process, the molten core is quenched to a glassy state as the fiber cools. Fibers were drawn to a total diameter of 125 μm and a conventional acrylate coating was applied yielding a total fiber diameter of about 250 μm.

Cross-sectional compositional analysis was conducted using Energy Dispersive x-ray (EDX) spectroscopy on a Hitachi SU-6600 scanning electron microscope (SEM) at a beam acceleration voltage of 15kV.

Refractive index profiles (RIPs) were measured transversely through the side of the fibers using a spatially resolved Fourier transform interferometer [14]. Attenuation was measured at a wavelength of 1550 nm using the standard cutback method. Brillouin gain coefficients (BGC) were determined by collecting the spontaneous Brillouin signal while pumping roughly 2 meters of fiber at a wavelength of 1534 nm using a narrow linewidth seed source. The BGC was estimated for each fiber by comparing the strength of the spontaneous scattering with a fiber of known BGC. A previously reported sapphire-derived fiber [11] was used to determine the Sellmeier coefficients for the alumina (Al_2O_3) component by using accepted additive models [12]. Estimated total dispersion curves were formulated using the RIP and the Sellmeier coefficients determined from the additive model.

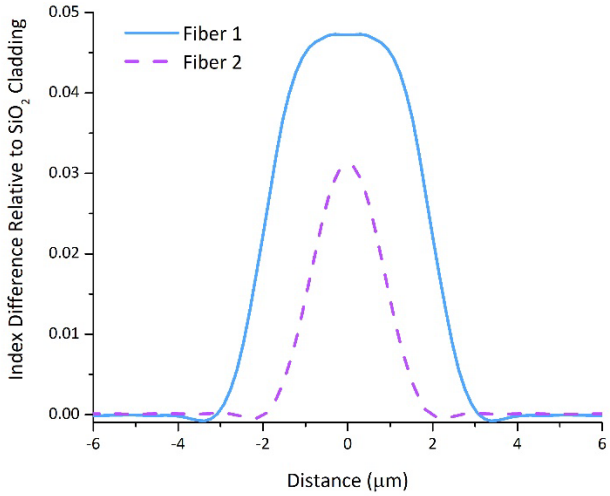

Fig. 2. Refractive index profile (RIP) for Fiber 1 and Fiber 2.

The nonlinear refractive index (n_2) of the two fibers was estimated using self-phase modulation (SPM) whereby a temporally short pulse with up to 1 kW of peak power at 1542 nm was launched into one end of 5-meter fiber segments. The output spectrum then was modeled using the standard nonlinear Schrödinger Equation and fit to the measured SPM spectra by adjusting the nonlinear coefficient. The estimate of n_2 allows for the determination of the Brillouin Figure of Merit (BFOM), defined as $BFOM = \gamma L_{eff} P_{th}$ [15] where γ is the nonlinear coefficient ($\gamma = 2\pi n_2/\lambda A_{eff}$ with λ being the optical wavelength), L_{eff} is the effective length (taking attenuation into consideration), and P_{th} is the SBS threshold power. If P_{th} is defined as in [16], then $L_{eff}P_{th} = 21A_{eff}/g_B$ and a simplified form is obtained: $BFOM = 42\pi n_2/\lambda g_B$. The $L_{eff}P_{th}$ prefactor value of 21 is known to vary depending on the shape of the Brillouin gain spectrum, but offers a reasonable approximation in the present case.

Figure 1 provides (a) a representative scanning electron microscope image of Fiber 2 magnified 700x and (b) magnified 6000x. Figure 2 provides the refractive index profiles (RIP) for the two fibers fabricated. Table 1 complements this by providing a summary of their physical properties. The effective area of the fibers is presented, though identifying the core diameter is somewhat subjective given the compositional gradient from the core center to the silica cladding. Accordingly, defining the core edge is limited by the resolution of the SEM compositional detection. Molar compositions (%) for the two fibers taken at the core center are presented in Table 1. The two fibers were drawn from the same preform. The beginning part of the draw had a shorter time at high temperature, resulting in larger core with less

dissolution of the core composition by cladding SiO_2 (Fiber 1). A longer equilibration time, i.e., towards the end of the draw, resulted in a fiber with concomitantly less Al_2O_3 and Y_2O_3 (Fiber 2). Given the influence of Al_2O_3 [11] and YAG [12] precursors on the refractive index of silica, and considering the measured Δn values, the concentration of SiO_2 would have been expected to be much lower in the fibers. Using data found in [12], along with the concentrations in Table 1, Δn for Fiber 2, for example, is calculated to be 29.8×10^{-3}; much lower than the measured value. This is attributed to the collection radius of the electron beam being larger than the core radius, so while analyzing the core center, the instrument detects and counts the surrounding silica. Also provided in Table 1 are the attenuation coefficients. Although they are relatively high, it is believed that the loss originates from the industrial-grade precursors, which are not optimized for purity. This is further evidenced since Fiber 2, consisting of a higher concentration of high-purity silica (lower Δn) resulting from the telecommunications-grade preform, yielded a lower attenuation.

Table 1. Summary of physical properties of two fabricated fibers

Parameter	Fiber 1	Fiber 2
Effective Area, A_{eff}* (μm², 1550 nm)	11.2	20.7
Δn (x10^{-3}) at core center	47.3	32.9
Al_2O_3 (mole%) at core center	9.16	6.95
Y_2O_3 (mole%) at core center	1.60	1.23
Yb_2O_3 (mole%) at core center	0.21	0.41
SiO_2 (mole%) at core center	89.13	91.41
BGC (x10^{-11} m/W)	0.125	0.139
n_2** (x10^{-20} m²/W)	1.8	2.0
Attenuation (dB/m, 1550 nm)	0.78	0.47
Dispersion* (ps/nm-km)	+9.0	-40.1
BFOM (1550 nm)	1.23	1.22

*Calculated from the refractive index profile (RIP)
**Estimated from SPM-based measurements

The Brillouin gain spectra for the two fibers are provided in Figure 3. The peak near 11 GHz and the smaller peak near 11.1 GHz are characteristic signatures of the measurement apparatus. Their amplitudes do not represent a true value for a gain coefficient of any fiber in the system. The Brillouin gain spectrum for Fiber 1 has a spectral width of about 200 MHz while that for Fiber 2 spans roughly 500 MHz. A significant amount of this broadening is related to increased acoustic attenuation brought on by acoustic wave anti-guidance resulting from the very small core diameter that has an acoustic velocity larger than the surrounding cladding. The sharp peak near the low-frequency end of the Fiber 2 spectrum is associated with Brillouin scattering in the cladding, which ultimately defines the SBS threshold for this fiber. Fiber 2 has a lower BGC due to the fundamental optical mode being more tightly confined. It is worthy to reiterate that it is precisely the small core diameter that has introduced the large-scale waveguide attenuation to the acoustic wave in the present case. This is in contrast to fibers with larger core diameters, but fabricated from similar materials, wherein the Brillouin gain coefficient is dominated primarily by material properties [17, 18], including material damping and low photoelastic constant.

The Sellmeier coefficients for the alumina component of the core glass composition are presented in Table 2. Direct measurements of the dispersion coefficients were unsuccessful due to the relatively high attenuation in the fiber. Accordingly, the optical dispersion was estimated from the RIPs and the deduced Sellmeier coefficients. This is shown in Figure 4. Fiber 1 portrays a normal dispersion until approximately a wavelength of about 1.4 μm after which it exhibits anomalous dispersion. Fiber 2 exhibits all-normal dispersion in the range of the calculation with a zero-dispersion point calculated to be approximately 2.0 μm.

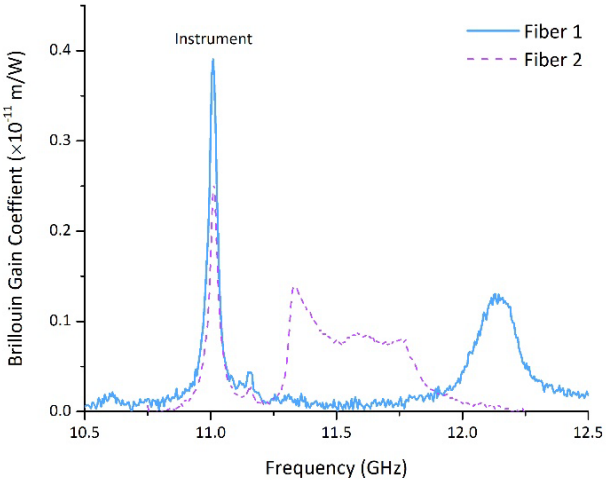

Fig. 3. Brillouin gain spectrum for Fiber 1 and Fiber 2.

As an example, Figure 5 provides the measured and calculated SPM spectrum for Fiber 2 at a pulse power of 850 W. The n_2 values deduced are somewhat lower than expected for aluminosilicate glasses [19].

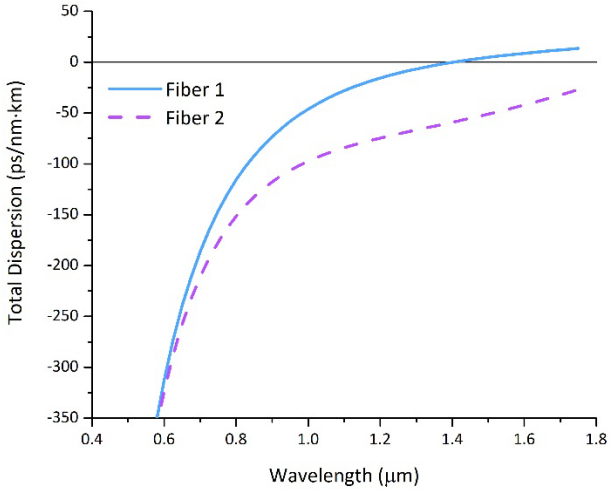

Fig. 4. Total Dispersion curves calculated from the RIP and deduced Sellmeier coefficients for Fiber 1 (solid line) and Fiber 2 (dashed line).

Table 2. Sellmeier coefficients for amorphous Al_2O_3 as deduced from an aluminosilicate optical fiber

A_1	2.4989×10^{-9}
l_1^2 (nm^2)	52575.7
A_2	0.14498
l_2^2 (nm^2)	17018.5
A_3	1.58869
l_3^2 (nm^2)	11645.0

At 20 mole percent of Al_2O_3, n_2 is expected to be about 25% larger than the pure silica value [20]. The previously estimated dispersion curves are the primary source for uncertainty for the n_2 values since the dispersion curves were estimated considering only the alumina contribution. That said, the 5m length of fiber employed in the SPM experiment, which is either close to or shorter than the predicted dispersion length. Accordingly, the unknown dispersion should not result in too large of an error. The BFOM determined from the estimated n_2 values was 1.23 (Fiber 1) and 1.22 (Fiber 2). Due to the very low intrinsic BGC, which was 13 dB lower than standard telecommunication optical fiber, both fibers have similar BFOM values that are comparable to those realized for both Ge- and Al-doped fibers with 1 kg of axially-gradient applied strain [2]. It is believed that n_2 values deduced from an experimentally obtained dispersion curve will be even higher than the estimated values presented, increasing the BFOM further.

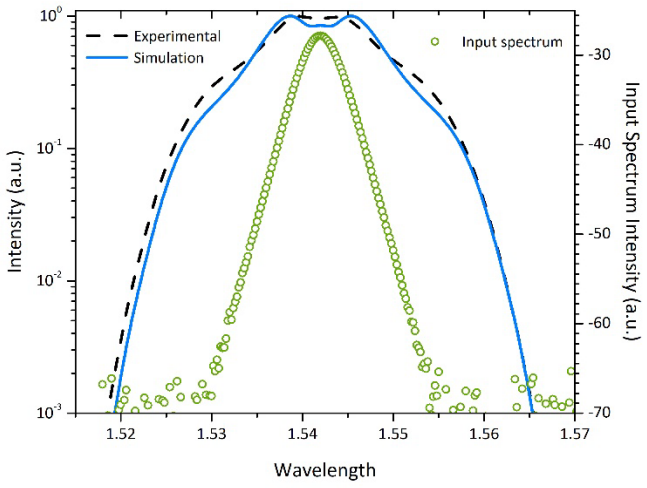

Fig. 5. Self-phase modulation spectrum, which was used to estimate the value of n_2 for Fiber 2 at a pulse power of 850 W.

In conclusion, a multilayer precursor core comprising of a Yb:YAG crystal rod inside of a sapphire sleeve and drawn into a small core diameter high-NA silica-clad optical fiber, exhibited exceptionally low intrinsic Brillouin gain coefficient of 0.125×10^{-11} m/W (Fiber 1) and 0.139×10^{-11} m/W (Fiber 2). These values are, respectively, 13 dB and 12.5 dB, lower than conventional optical fiber. Stimulated Brillouin scattering (SBS) is cladding-limited in Fiber 2, but it is believed further reductions in BGC are possible. Tradeoffs exist between the core diameter, NA, strength of n_2 nonlinearity, and the Brillouin gain coefficient that still need to be optimized. The measured n_2 is lower than expected and approximately that for pure silica. Further, the effects of the yttria (Y_2O_3) and ytterbia (Yb_2O_3) components on the n_2 of the fiber still need to be considered. Moreover, the low-silica content, and the resulting enhanced coefficient of thermal expansion relative to the pure silica cladding, may play a role in fiber performance through the introduction of stresses during fiber draw, warranting further investigation. Direct measurements of the dispersion coefficient remain unsuccessful due to the attenuation in the fiber. Reducing the attenuation in these fibers should allow for more accurate measurements of the BGC as well as the dispersion coefficient which ultimately leads to a more accurate n_2. Introducing precursor components optimized for purity may reduce present losses, potentially allowing for more accurate measurements to be conducted.

Acknowledgment. The authors thank Dr. Andrew Yablon (Interfiber Analysis, LLC) for the refractive-index measurements and Donald Mulwee (Clemson University) for electron microscopy support. Financial support from the US Department of Defense High Energy Laser Joint Technology Office (HEL JTO) through contract N00014-17-1-2546 and the J. E. Sirrine Foundation (CK, TH, and JB) also are gratefully acknowledged.

References

1. G. Mélin, D. Labat, L. Galkovsky, A. Fleureau, S. Lempereur, A. Mussot, and A. Kudlinski, Electron. Lett. **48**, 232 (2012).
2. C. Lundström, R. Malik, L. Grüner-Nielsen, B. Corcoran, S.L.I. Olsson, M. Karlsson, and P.A. Andrekson, IEEE Photon. Technol. Lett. **25**, 234 (2013).
3. S.-S. Lin, S.-K. Hwang, and J.-M. Liu, Opt. Express **22**, 4152 (2014).
4. S. K. Korotky, P. B. Hansen, L. Eskildsen, and J. J. Veselka, in Proc. Technol. Dig. Conf. Integr. Opt. Fiber Commun., 1995, p. 110.
5. J. M. C. Boggio, J. D. Marconi, and H.L. Fragnito, J. Lightwave Technol. **23**, 3808 (2005).
6. Y. Takushima and T. Okoshi, Electron. Lett. **28**, 1155 (1992).
7. T. Nakanishi, M. Tanaka, T. Hasegawa, M. Hirano, T. Okuno, and M. Onishi, in Proc. ECOC 2006, Cannes, France, vol. 6, p. 17, Paper TH.4.2.2.
8. P.D. Dragic, C.-H. Liu, G.C. Papen, and A. Galvanauskas, CLEO Technical Digest, paper CThZ3 (2005).
9. C.K. Jen, Proc. IEEE Ultrasonics Symp., 1128 (1985).
10. P.D. Dragic, presented at the IEEE Photonics Society Summer Topicals Meeting, paper TuC3.2, 19 July 2010.
11. P. Dragic, T. Hawkins, P. Foy, S. Morris, and J. Ballato, Nat. Photon. **6**, 627 (2012).
12. J. Ballato and P. Dragic, J. Am. Ceram. Soc. **96**, 2675 (2013).
13. P.D. Dragic, P.-C. Law, and Y.-S. Liu, Microw. Opt. Technol. Lett. **54**, 2347 (2012).
14. A. D. Yablon, J. Lightwave Technol. **28**, 360 (2010).
15. L. Grüner-Nielsen, S. Herstrom, S. Dasgupta, D. Richardson, D. Jakobsen, C. Lundström, P.A. Andrekson, M.E.V. Pederson, and B. Pálsdóttir, IEEE Winter Topicals (WTM) 2011, paper MD3.2.
16. R. G. Smith, Appl. Opt. **11**, 2489, (1972).
17. P.D. Dragic, C. Kucera, J. Ballato, D. Litzkendorf, J. Dellith, and K. Schuster, Appl. Opt. **53**, 5660 (2014).
18. P. Dragic, P.-C. Law, J. Ballato, T. Hawkins, and P. Foy, Opt. Express **18**, 10055 (2010).
19. T. Kato, Y. Suetsugu, M. Takagi, E. Sasaoka, and M. Nishmura, Opt. Lett. **20**, 988 (1995).
20. P. Dragic, M. Cavillon, and J. Ballato, Int. J. Appl. Glass Sci. (submitted 2017).

References

1. G. Mélin, D. Labat, L. Galkovsky, A. Fleureau, S. Lempereur, A. Mussot, and A. Kudlinski, "Highly-nonlinear photonic crystal fiber with high figure of merit around 1 µm," *Electronic Letters* **48**, 232-234 (2012).
2. C. Lundström, R. Malik, L. Grüner-Nielsen, B. Corcoran, S.L.I. Olsson, M. Karlsson, and P.A. Andrekson, "Fiber Optic Parametric Amplifier With 10-dB Net Gain Without Pump Dithering," *IEEE Photonic Technology Letters* **25**, 234-237 (2013).
3. S.-S. Lin, S.-K. Hwang, and J.-M. Liu, "Supercontinuum generation in highly nonlinear fibers using amplified noise-like optical pulses," *Optics Express* **22**, 4152-4160 (2014).
4. S. K. Korotky, P. B. Hansen, L. Eskildsen, and J. J. Veselka, "Efficient phase modulation scheme for suppressing stimulated Brillouin scattering," in Proc. Technol. Dig. Conf. Integr. Opt. Fiber Commun., 1995, pp. 110–111.
5. J. M. C. Boggio, J. D. Marconi, and H.L. Fragnito, "Experimental and numerical investigation of the SBS-threshold increase in an optical fiber by applying strain distributions," *Journal of Lightwave Technology* **23**, 3808–3814 (2005).
6. Y. Takushima and T. Okoshi, "Suppression of simulated Brillouin scattering using optical isolators," *Electronic Letters* **28**, 1155–1157 (1992).
7. T. Nakanishi, M. Tanaka, T. Hasegawa, M. Hirano, T. Okuno, and M. Onishi, "AlO-SiO core highly nonlinear dispersion-shifted fiber with Brillouin gain suppression improved by 6.1 dB," in Proc. ECOC 2006, Cannes, France, vol. 6, pp. 17–18, Paper TH.4.2.2.
8. P.D. Dragic, C.-H. Liu, G.C. Papen, and A. Galvanauskas, "Optical Fiber with an Acoustic Guiding Layer for Stimulated Brillouin Scattering Suppression," CLEO Technical Digest, paper CThZ3 (2005).
9. C.K. Jen, "Similarities and differences between fiber acoustics and fiber optics," Proc. IEEE Ultrasonics Symp., 1128–33 (1985).
10. P.D. Dragic, "Brillouin suppression by fiber design," presented at the IEEE Photonics Society Summer Topicals Meeting, paper TuC3.2, 19-21 July 2010.
11. P. Dragic, T. Hawkins, P. Foy, S. Morris, and J. Ballato, "Sapphire-derived all-glass optical fibers," *Nature Photonics* **6**, 627-633 (2012).
12. J. Ballato and P. Dragic, "Rethinking Optical Fiber: New Demands, Old Glasses," *Journal of the American Ceramic Society* **96**, 2675-2692 (2013).
13. P.D. Dragic, P.-C. Law, and Y.-S. Liu, "Higher order modes in acoustically antiguiding optical fiber," *Microwave and Optical Technology Letters* **54**, 2347-2349 (2012).
14. A. D. Yablon, "Multi-wavelength optical fiber refractive index profiling by spatially resolved Fourier transform spectroscopy," *Journal of Lightwave Technology* **28**, 360-364 (2010).
15. L. Grüner-Nielsen, S. Herstrom, S. Dasgupta, D. Richardson, D. Jakobsen, C. Lundström, P.A. Andrekson, M.E.V. Pederson, and B. Pálsdóttir, "Silica-Based Highly Nonlinear Fibers with a High SBS Threshold," IEEE Winter Topicals (WTM) 2011, paper MD3.2.
16. R.G. Smith, "Optical Power Handling Capacity of Low Loss Optical Fibers as Determined by Stimulated Raman and Brillouin Scattering," *Applied Optics* **11**, 2489-2494 (1972).
17. P.D. Dragic, C. Kucera, J. Ballato, D. Litzkendorf, J. Dellith, and K. Schuster, "Brillouin scattering properties of lanthano-aluminosilicate optical fiber," Applied Optics **53**, 5660-5671 (2014).
18. P. Dragic, P.-C. Law, J. Ballato, T. Hawkins, and P. Foy, "Brillouin spectroscopy of YAG-derived optical fibers," Optics Express **18**, 10055-10067 (2010).
19. T. Kato, Y. Suetsugu, M. Takagi, E. Sasaoka, and M. Nishmura, "Measurement of the nonlinear refractive index in optical fiber by the cross-phase-modulation method with depolarized pump light," *Optics Letters* **20**, 988-990 (1995).
20. P. Dragic, M. Cavillon, and J. Ballato, "The linear and nonlinear refractive index of amorphous Al_2O_3 deduced from aluminosilicate optical fibers," *International Journal of Applied Glass Science* (submitted 2017).